Title

Hepatic Transcriptome and Its Regulation Following Soluble Epoxide Hydrolase Inhibition in Alcohol-Associated Liver Disease

Journal

American Journal Of Pathology, 194(1)

ISSN

0002-9440

Authors

Warner, Jeffrey B

Hardesty, Josiah E

Song, Ying L

et al.

Publication Date

2024

DOI

10.1016/j.ajpath.2023.09.016

Peer reviewed

The American Journal of Pathology, Vol. 194, No. 1, January 2024

ELSEVIER

The American Journal of PATHOLOGY

ajp.amjpathol.org

GASTROINTESTINAL, HEPATOBILIARY, AND PANCREATIC PATHOLOGY

Hepatic Transcriptome and Its Regulation Following Soluble Epoxide Hydrolase Inhibition in Alcohol-Associated Liver Disease

Jeffrey B. Warner,[*†] Josiah E. Hardesty,[*†] Ying L. Song,[*] Alison T. Floyd,[*] Zhongbin Deng,[‡§] Audriy Jebet,[¶] Liqing He,[¶] Xiang Zhang,[¶] Craig J. McClain,[*†‖**††] Bruce D. Hammock,[‡‡] Dennis R. Warner,[*] and Irina A. Kirpich[*†‖**§§]

From the Division of Gastroenterology, Hepatology, and Nutrition, Department of Medicine, the Department of Pharmacology and Toxicology,† the University of Louisville Alcohol Center,‖ the University of Louisville Hepatobiology & Toxicology Center,** and the Department of Microbiology and Immunology,§§ University of Louisville School of Medicine, Louisville, Kentucky; the Division of Immunotherapy,‡ Department of Surgery, the Brown Cancer Center,§ and the Department of Chemistry,¶ University of Louisville, Louisville, Kentucky; the Robley Rex Veterans Medical Center,†† Louisville, Kentucky; and the Department of Entomology and Nematology,‡‡ Comprehensive Cancer Center, University of California, Davis, California*

Accepted for publication September 27, 2023.

Address correspondence to Irina A. Kirpich, Ph.D., M.P.H., Department of Microbiology and Immunology, University of Louisville, 505 Hancock St., Louisville, KY 40202. E-mail: irina.kirpich@louisville.edu.

Alcohol-associated liver disease (ALD) is a serious public health problem with limited pharmacologic options. The goal of the current study was to investigate the efficacy of pharmacologic inhibition of soluble epoxide hydrolase (sEH), an enzyme involved in lipid metabolism, in experimental ALD, and to examine the underlying mechanisms. C57BL/6J male mice were subjected to acute-on-chronic ethanol (EtOH) feeding with or without the sEH inhibitor 4-[[*trans*-4-[[[[4-trifluoromethoxy phenyl]amino] carbonyl]-amino]cyclohexyl]oxy]-benzoic acid (TUCB). Liver injury was assessed by multiple end points. Liver epoxy fatty acids and dihydroxy fatty acids were measured by targeted metabolomics. Whole-liver RNA sequencing was performed, and free modified RNA bases were measured by mass spectrometry. EtOH-induced liver injury was ameliorated by TUCB treatment as evidenced by reduced plasma alanine aminotransferase levels and was associated with attenuated alcohol-induced endoplasmic reticulum stress, reduced neutrophil infiltration, and increased numbers of hepatic M2 macrophages. TUCB altered liver epoxy and dihydroxy fatty acids and led to a unique hepatic transcriptional profile characterized by decreased expression of genes involved in apoptosis, inflammation, fibrosis, and carcinogenesis. Several modified RNA bases were robustly changed by TUCB, including N^6-methyladenosine and 2-methylthio-N^6-threonylcarbamoyladenosine. These findings show the beneficial effects of sEH inhibition by TUCB in experimental EtOH-induced liver injury, warranting further mechanistic studies to explore the underlying mechanisms, and highlighting the translational potential of sEH as a drug target for this disease. *(Am J Pathol 2024, 194: 71–84; https://doi.org/10.1016/j.ajpath.2023.09.016)*

Alcohol-associated liver disease (ALD) is a common liver disease resulting from excessive chronic alcohol consumption. This condition contributes to nearly one-half of liver cirrhosis–related deaths worldwide[1] and poses a major health care, societal, and economic burden. ALD is a spectrum of liver disease states that ranges from simple steatosis, a manifestation present in nearly all heavy drinkers, to steatohepatitis, liver fibrosis, cirrhosis, and hepatocellular carcinoma. Binge drinking superimposed on chronic alcohol consumption in some individuals may lead to alcohol-associated hepatitis (AH), an acute condition with

Supported by the NIH through multiple research grants, including: R01AA024102-01A1 (I.A.K.); U01AA026934, 1U01AA026926-01, 1U01AA026980-01, and R01AA023681 (C.J.M.); 5T32ES011564-15 and 1F31AA028423-01A1 (J.B.W.); F32AA027950-01A1 and K99AA030627 (J.E.H.); and P42ES004699 (B.D.H.); and by the Jewish Healthcare Foundation for Excellence Research Enhancement Grant Program at the University of Louisville (I.A.K.), an Institutional Development Award from the NIH National Institute of General Medical Sciences under grant P20GM113226 (C.J.M.), and the NIH National Institute on Alcohol Abuse and Alcoholism under grant P50AA024337 (C.J.M.).

https://doi.org/10.1016/j.ajpath.2023.09.016

a high degree of morbidity and mortality.[2] There is no US Food and Drug Administration–approved therapy for any stage of ALD, including AH. The current pharmacologic options for AH are limited to corticosteroids such as prednisolone, which only modestly improve mortality at the cost of dangerous immunosuppression in some individuals.[3] Alternatively, only a fraction of individuals with AH receive liver transplants, and these individuals can accrue total health care costs exceeding $1 million.[4] Clearly, there is an urgent need for the development of novel therapeutic strategies for patients with ALD, particularly those with AH.

Accumulating evidence from experimental animal studies suggests that inhibition of soluble epoxide hydrolase (sEH) is a promising therapeutic strategy in various disease models, including liver pathologies such as steatosis, fibrosis, and portal hypertension (reviewed elsewhere[5]). sEH is a metabolic enzyme responsible for the hydrolysis of epoxy fatty acids (EpFAs), metabolites of various polyunsaturated fatty acids, to form dihydroxylated fatty acids (DhFAs).[6,7] EpFAs are generally anti-inflammatory, analgesic, pro-regenerative lipid mediators exerting their beneficial biological effects via several receptors, including peroxisome proliferator–activated receptors,[8,9] prostaglandin receptors, and cAMP signaling via G protein–coupled receptors.[10] By blocking sEH activity, sEH inhibitors prevent the degradation of EpFAs and potentially limit production of DhFAs, which are generally considered to be biologically inactive, less active, or, in some cases, deleterious.[11,12] A recent study found that heavy-drinking individuals with severe ALD had elevated plasma levels of the linoleic acid–derived DhFAs 9,10-DiHOME and 12,13-DiHOME and, subsequently, corresponding elevated DhFA/EpFA ratios (an indirect marker of increased sEH activity), compared with healthy control subjects or patients who were heavy drinkers with or without mild liver injury.[13] Studies in experimental animal models of ALD showed that genetic ablation of liver sEH ameliorated ethanol (EtOH)-induced hepatic steatosis, injury, inflammation, and oxidative and endoplasmic reticulum (ER) stress.[14] This evidence from clinical and experimental ALD supported the role of sEH in ALD pathogenesis and suggests that pharmacologic sEH inhibition might be an effective therapeutic strategy to attenuate ALD.

The aim of the current study was to investigate the efficacy of the sEH inhibitor 4-[[*trans*-4-[[[[4-trifluoromethoxy phenyl]amino]carbonyl]-amino]cyclohexyl]oxy]-benzoic acid (TUCB) in experimental ALD and to examine the underlying mechanisms, including the effects on liver transcriptional changes and transcriptional regulatory mechanisms.

Materials and Methods

Mice

Male C57BL/6J mice were purchased from The Jackson Laboratory (Bar Harbor, ME) and housed in a specific pathogen–free animal facility accredited by the Association for Assessment and Accreditation of Laboratory Animal Care. The room was maintained on a 12-hour light/dark cycle. All animal studies were conducted under a protocol approved by the University of Louisville Institutional Animal Care and Use Committee.

Animal Model

The study used a well-established National Institute on Alcohol Abuse and Alcoholism mouse model of ALD (a model of chronic-binge or acute-on-chronic EtOH exposure)[15] wherein 8- to 10-week–old C57BL/6J male were provided a 5% (v/v) EtOH-containing all-liquid Lieber-DeCarli diet for 10 days followed by a single EtOH "binge" on day 11, delivered by oral gavage (5 g/kg) 9 hours before euthanasia. The control and EtOH liquid Lieber-DeCarli diets (F1259SP and F1258SP, respectively) were purchased from Bio-Serv (Flemington, NJ). The EtOH and control diets were isocaloric, wherein maltodextrin was substituted for EtOH in the control diet. A subset of mice received the sEH inhibitor TUCB, which was added to the liquid diet.

There are a number of sEH inhibitors of varying potencies and properties, including 1-trifluoromethoxyphenyl-3-(1-propionylpiperidin-4-yl) urea (TPPU), which was previously used in a similar National Institute on Alcohol Abuse and Alcoholism mouse model of ALD.[14] Because TPPU exhibited a limited effect on liver steatosis and injury in EtOH-fed mice in that study, we selected TUCB for the current study owing to its greater potency in mice (half-maximal inhibitory concentration, TUCB 5.7 nmol/L[16] vs TPPU 90 nmol/L[17]). In addition, TUCB has previously shown efficacy in a number of models of liver pathology, including liver fibrosis[18] and portal hypertension.[19] TUCB was dissolved in a small volume of vehicle EtOH and then added to the liquid diet at a concentration of 7.5 μg/mL, which was estimated to deliver a dose of 3 mg/kg per day per mouse. This dose was chosen based on a pilot study in mice showing its highest efficacy on EtOH-induced liver injury in mice (unpublished data). Vehicle control animals received an equivalent volume of EtOH (0.19% v/v EtOH). There were four experimental groups: pair-fed (PF) + vehicle, PF + TUCB, EtOH + vehicle, and EtOH + TUCB. At the termination of the experiment, mice were deeply anesthetized with 100 mg/kg ketamine/16 mg/kg xylazine, and blood was collected from the inferior vena cava into heparinized syringes. The plasma fraction was prepared by centrifugation at 2000 × *g* for 10 minutes, aliquoted, and stored at −80°C for further analysis. Portions of liver tissue from the left hepatic lobe were snap-frozen in liquid nitrogen and stored at −80°C or were fixed in 10% neutral buffered formalin and embedded in paraffin for histologic assessment.

Alanine Aminotransferase Measurement

Plasma alanine aminotransferase (ALT) levels were measured as a biomarker of liver injury using the ALT/

glutamic pyruvic transaminase reagent as per the manufacturer's instructions (Thermo Fisher Scientific, Waltham, MA).

Blood Alcohol Concentration

Blood alcohol concentration was determined in plasma by using the EnzyChrom ethanol assay kit (BioAssay Systems, Hayward, CA) according to the manufacturer's instructions.

Liver Tissue Staining and Assessment

Formalin-fixed, paraffin-embedded liver sections were cut to 5 μm thickness, then stained with hematoxylin and eosin for assessment of gross hepatic pathology. Neutrophil accumulation in the livers was assessed by chloroacetate esterase staining using a commercially available kit (Sigma Chemical, St. Louis, MO) according to the manufacturer's instructions. Quantification of chloroacetate esterase staining was performed via light microscopy by blindly quantifying positive cells in 10 to 20 random digital images (×200 magnification) per liver section ($n = 5$ to 10 sections per group) by two independent investigators. Positive cells were then averaged between images to obtain an average per mouse.

Liver Triglycerides and Free Fatty Acids

Hepatic lipids were extracted with chloroform and methanol as previously described.[20] Triglycerides and free fatty acids were measured by using the Infinity Triglycerides and Non-Esterified Fatty Acids kits (Thermo Fisher Scientific), respectively.

Liver Targeted Lipidomics

Snap-frozen liver samples were provided to the Wayne State University Lipidomics Core Facility (Detroit, MI) for targeted polyunsaturated fatty acid metabolite analysis as previously described.[13]

Western Blot Analysis

Liver tissue sample preparation for Western blot analysis was performed as previously described.[21] Antibodies used were anti-CHOP (Cell Signaling Technology, Danvers, MA; clone D46F1) and anti−β-actin (Santa Cruz Biotechnology, Dallas, TX).

Myeloperoxidase Activity

Liver homogenates were prepared in phosphate-buffered saline and assayed for myeloperoxidase activity as described by the manufacturer (Cell Biolabs, San Diego, CA). Data were normalized to total protein as measured by using the bicinchoninic acid assay (Thermo Scientific Scientific).

Liver Immune Cell Isolation and Flow Cytometry Analysis

Immune cells were isolated from mice subjected to the National Institute on Alcohol Abuse and Alcoholism chronic-binge EtOH exposure model. Analysis of immune cell phenotypes was performed as described previously.[22,23]

Liver mRNA Sequencing and Analysis

Liver samples were provided to Azenta Life Sciences (South Plainfield, NJ) for RNA extraction followed by 150 bp paired-end standard RNA sequencing analysis via the HiSeq system (Illumina, San Diego, CA). Differentially expressed (DE) genes were identified via DESeq2[24] as defined by a Wald test adjusted P value <0.05 and absolute $\log_2$ fold change >1. Gene ontology analysis was performed in-house using Cytoscape version 3.9.1.[25] Heatmap analysis of RNA sequencing data was performed using Heatmapper Expression (*http://www.heatmapper.ca*, last accessed July 20, 2023) followed by average linkage and Pearson hierarchical clustering to identify gene expression patterns across experimental groups.

RNA sequencing data are available under European Nucleotide Archive project accession number PRJEB63137 (*https://www.ebi.ac.uk/ena*, last accessed October 1, 2023).

Extraction and Measurement of Free Modified Nucleosides

Free nucleosides and bases were extracted from whole-liver lysates as previously described.[26] Targeted measurement was performed by liquid chromatography/mass spectroscopy using a Thermo Q Exactive HF Hybrid Quadrupole-Orbitrap Mass Spectrometer paired with a Thermo DIONEX UltiMate 3000 HPLC system (Thermo Fisher Scientific) paired with a reversed-phase chromatography column as previously described.[26,27] The analysis was performed by the University of Louisville Alcohol Center Metabolomic/Lipidomic Core.

Statistical Analysis

Data are expressed as means ± SEM. GraphPad Prism version 9.3.1 (GraphPad Software, La Jolla, CA) was used to perform t-tests or one-way analysis of variance tests with the Šidák multiple comparisons test for data following a normal distribution and the Mann-Whitney and Kruskal-Wallis H tests for data following a non-normal distribution. Data were considered significant at $P < 0.05$. Principal component analysis (PCA) was performed in GraphPad Prism 9.3.1, and results were then visualized using the plot3D function of the rgl package (*https://github.com/dmurdoch/rgl* and *https://dmurdoch.github.io/rgl*) in RStudio version 1.3.1093 (PBC, Boston, MA) running R version 4.0.3 (R Foundation for Statistical Computing, Vienna, Austria). Heatmaps were

constructed using MetaboAnalyst freeware (MetaboAnalyst, *https://www.metaboanalyst.ca*, last accessed July 20, 2023).

Results

sEH Inhibition Prevents Liver Injury in a Mouse Model of ALD

Chronic-binge EtOH exposure robustly increased plasma ALT levels in experimental mice, and TUCB treatment significantly alleviated this increase (Figure 1A), suggesting beneficial effects of sEH inhibition on liver injury caused by EtOH administration in this ALD animal model. In contrast, EtOH-induced hepatic steatosis was not affected by TUCB as determined by liver histologic analysis, triglyceride levels, and free fatty acid measurement (Figure 1, B and C, and Table 1). No significant effects of TUCB were detected on body weight gain, food consumption, or blood alcohol concentration (Table 1). To further characterize the liver phenotype in response to TUCB treatment in EtOH-fed mice, common features of ALD such as neutrophil infiltration,[28] macrophage phenotype,[29] oxidative stress,[30] and ER stress[31] were evaluated. As expected, EtOH administration resulted in significantly elevated hepatic neutrophil infiltration as evidenced by chloroacetate esterase staining (Figure 1, D and E) and increased myeloperoxidase activity, an enzyme that is primarily expressed by neutrophils (Figure 1F). However, TUCB treatment had a limited effect on both of these markers in EtOH-fed mice. Furthermore, compared with EtOH alone, EtOH-fed mice treated with TUCB had a significantly increased number of M2-like major histocompatibility complex class II receptor $CD206^+$ macrophages, a tissue restorative phenotype,[32] as determined by flow cytometry analysis (Figure 1, G and H).

In line with the previously reported attenuation of ER stress by TPPU[14] in a similar animal model, TUCB led to a favorable effect on a marker of ER stress, specifically, the expression of CHOP, a transcription factor induced by ER stress and the convergent point for the three arms of the unfolded protein response. Indeed, mice fed EtOH had a significant increase in the expression of CHOP, which was significantly attenuated by TUCB (Figure 1, I and J). Interestingly, TUCB treatment had no effect on EtOH-induced liver malondialdehyde levels, an indirect marker of oxidative damage (Supplemental Figure S1A).

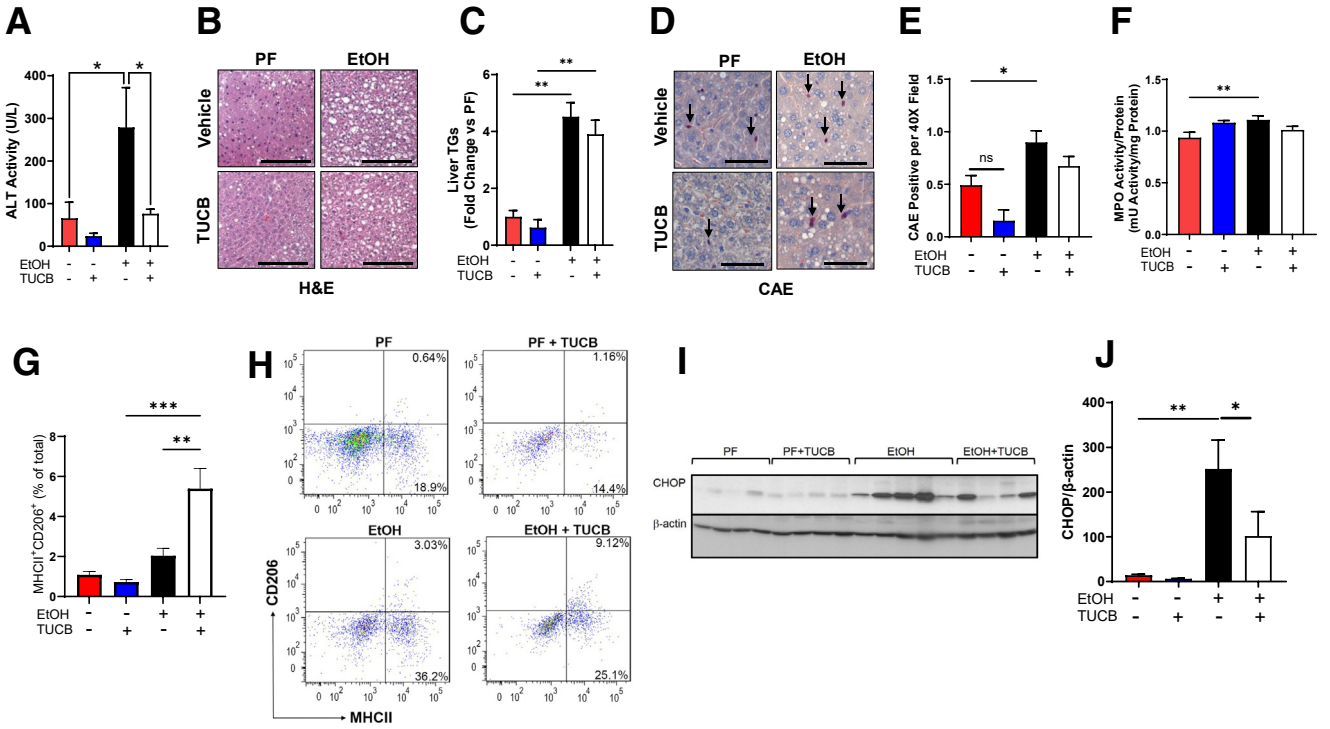

Figure 1 Inhibition of soluble epoxide hydrolase by 4-[[*trans*-4-[[[[4-trifluoromethoxy phenyl]amino]carbonyl]-amino]cyclohexyl]oxy]-benzoic acid (TUCB) attenuates acute-on-chronic ethanol (EtOH)-associated liver injury in mice. **A:** Plasma alanine aminotransferase (ALT) activity. **B:** Representative liver hematoxylin and eosin (H&E)-stained sections. **C:** Liver triglyceride (TG) levels. **D:** Chloroacetate esterase (CAE) staining for neutrophils (positive cells indicated with **arrows**). **E:** Quantification of CAE-positive cells. **F:** Myeloperoxidase (MPO) activity in liver lysates. **G**—**H:** Quantitative analysis [percent frequencies of total major histocompatibility complex class II receptor ($MHCII^+$)$CD206^+$ cells] and representative contour plots indicating mean frequencies of the hepatic $MHCII^+CD206^+$ cells assessed by using flow cytometry. **I**—**J:** Western blot analysis and quantitation of hepatic CHOP expression, normalized to β-actin expression. Data are expressed as means ± SEM. $n = 5$ to 15 animals per group. $^*P < 0.05$, $^{**}P < 0.01$, $^{***}P < 0.001$ (comparisons with no asterisk were not statistically significant). Scale bars: 50 μm (**B and D**). Total magnification: ×400 (**B and D**). ns, not significant; PF, pair-fed.

Table 1 Metabolic Characteristics of PF, EtOH-fed, and TUCB-treated Mice

Characteristic	PF ($n = 5$)	PF + TUCB ($n = 5$)	EtOH ($n = 13$)	EtOH + TUCB ($n = 15$)	Analysis of variance *P* value
Metabolic measurements					
Initial BW, g	23.96 ± 1.15	23.84 ± 0.50	25.24 ± 0.30	26.03 ± 0.47†	0.0400
Final BW, g	26.10 ± 0.79	25.92 ± 0.81	24.30 ± 0.35	25.33 ± 0.59	0.1060
Liver/BW ratio, %	3.104 ± 0.679	4.091 ± 0.267	4.563 ± 0.121*	4.574 ± 0.037	0.0235
Fat/BW ratio, %	1.290 ± 0.284	1.745 ± 0.389	1.697 ± 0.201	1.571 ± 0.126	0.6324
Food consumption, g/d per mouse			9.100 ± 0.319	9.280 ± 0.404	0.8884
Biochemical measurements					
Liver triglycerides, mg/g liver	6.411 ± 1.414	3.955 ± 1.826	28.950 ± 3.208*	25.010 ± 3.181†	<0.0001
Liver free fatty acids, mEq/g liver	9.260 ± 0.678	10.640 ± 1.002	12.820 ± 0.612*	11.930 ± 0.581	0.0198
Blood alcohol concentration, mg/dL	nd	nd	412.33 ± 51.00	450.24 ± 58.74	0.6932

Data are expressed as means ± SEM. PF mice consume the same amount of food as EtOH-fed mice (pair-feeding paradigm).

*$P < 0.05$ for PF versus EtOH-fed mice.

†$P < 0.05$ for PF + TUCB versus EtOH + TUCB.

BW, body weight; EtOH, ethanol; nd, not determined; PF, paired-end; TUCB, 4-[[*trans*-4-[[[[4-trifluoromethoxy phenyl]amino]carbonyl]-amino]cyclohexyl]oxy]-benzoic acid.

ALD is often accompanied by mitochondrial dysfunction[33]; however, there was a limited effect of both EtOH and TUCB in EtOH-fed mice on mitochondria function in this animal model. Specifically, a modest decrease in the respiratory control ratio was observed in EtOH-treated and EtOH + TUCB–treated mice, with a concomitant increase in state 3 oxygen consumption (Supplemental Figure S1, B and C). Taking together, the obtained data show a beneficial effect of pharmacologic sEH inhibition by TUCB on EtOH-induced liver injury in experimental mice. TUCB treatment mitigated EtOH-induced hepatic ER stress and promoted a M2 macrophage phenotype, while having limited effects on hepatic steatosis, markers of neutrophil infiltration and oxidative stress, suggesting involvement of multiple mechanisms, and likely yet unknown molecules and signaling pathways mediating this favorable effect of TUCB on liver damage caused by acute-on-chronic EtOH exposure.

TUCB Treatment in EtOH-fed Mice Promotes a Shift of Hepatic Oxylipins Toward the PF Phenotype

The benefits of sEH inhibition, in part, are tied to the role of this enzyme in the metabolism of polyunsaturated fatty acid–derived lipid mediators; therefore, the levels of hepatic EpFAs and their cognate DhFAs were further evaluated. EtOH administration increased or decreased the levels of several hepatic polyunsaturated fatty acid–derived metabolites, many of which were reversed by TUCB administration, as visualized in the heatmap in Figure 2A. Specifically, TUCB administration reversed the EtOH-induced increase in 5,6-/8,9-DiHETrE:EpETrE and 9,10-DiHOME:EpOME ratios, as well as the overall combined DhFA:EpFA ratio. Raw values for all detected lipids and DhFA:EpFA ratios, where this calculation was possible, are provided in Table 2. PCA confirmed that EtOH feeding led to a significant divergence in the levels of these EpFAs and

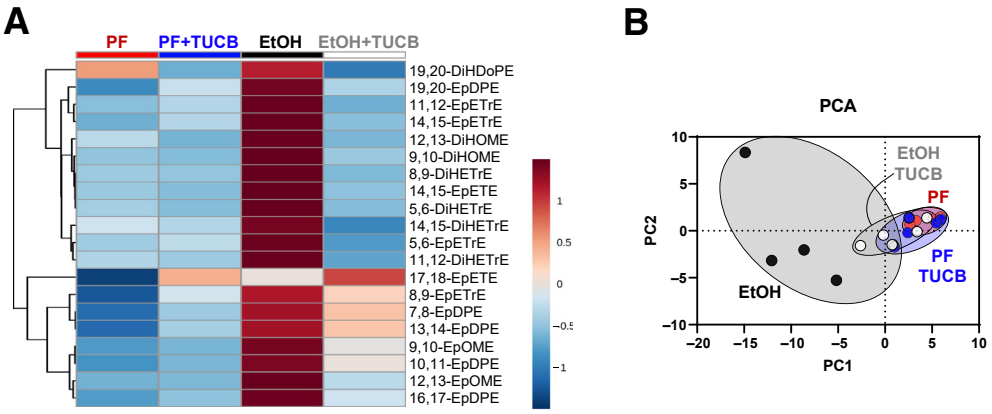

Figure 2 **A:** Heatmap with Ward clustering showing trends in individual hepatic polyunsaturated fatty acid metabolites (color scale represents *Z* score). **B:** Principal component analysis (PCA) of polyunsaturated fatty acid metabolites. $n = 5$ animals per group. EtOH, ethanol; PC1, first principal component; PC2, second principal component; PF, pair-fed; TUCB, 4-[[*trans*-4-[[[[4-trifluoromethoxy phenyl]amino]carbonyl]-amino]cyclohexyl]oxy]-benzoic acid.

Table 2 Liver Levels of PUFA Metabolites and Ratios ($n = 5$ per Group)

EpoxyFAs and dihydroxy FAs	PF ($n = 5$)	PF + TUCB ($n = 5$)	EtOH ($n = 5$)	EtOH + TUCB ($n = 5$)	Analysis of variance *P* value
9(10)-EpOME	0.625 ± 0.308	0.367 ± 0.118	0.864 ± 0.186	0.507 ± 0.129	0.375
12(13)-EpOME	0.322 ± 0.151	0.184 ± 0.052	0.686 ± 0.158	0.258 ± 0.059	0.035
5,6-EpETrE	0.034 ± 0.007	0.031 ± 0.010	0.0562 ± 0.013	0.0236 ± 0.008	0.154
8,9-EpETrE	0.012 ± 0.003	0.011 ± 0.003	0.021 ± 0.004	0.016 ± 0.005	0.273
11,12-EpETrE	0.060 ± 0.015	0.046 ± 0.013	0.135 ± 0.027	0.038 ± 0.015	0.010
14,15-EpETrE	0.030 ± 0.009	0.027 ± 0.006	0.057 ± 0.012	0.023 ± 0.007	0.056
14,15-EpETE	0.012 ± 0.003	0.010 ± 0.002	0.061 ± 0.016	0.010 ± 0.002	0.001
17,18-EpETE	0.003 ± 0.002	0.003 ± 0.001	0.004 ± 0.001	0.003 ± 0.001	0.847
7(8)-EpDPE	0.008 ± 0.004	0.003 ± 0.002	0.013 ± 0.002	0.012 ± 0.004	0.924
10(11)-EpDPE	0.035 ± 0.015	0.025 ± 0.009	0.064 ± 0.013	0.037 ± 0.009	0.151
13(14)-EpDPE	0.018 ± 0.010	0.015 ± 0.005	0.029 ± 0.004	0.021 ± 0.005	0.489
16(17)-EpDPE	0.013 ± 0.006	0.010 ± 0.003	0.033 ± 0.008	0.013 ± 0.004	0.041
19(20)-EpDPE	0.031 ± 0.017	0.025 ± 0.004	0.048 ± 0.010	0.023 ± 0.005	0.307
9,10-DiHOME	0.115 ± 0.051	0.054 ± 0.010	0.434 ± 0.251	0.072 ± 0.012	0.163
12(13)-DiHOME	0.150 ± 0.065	0.068 ± 0.008	0.184 ± 0.088	0.070 ± 0.013	0.372
5,6-DiHETrE	0.008 ± 0.002	0.005 ± 0.001	0.061 ± 0.036	0.005 ± 0.000	0.108
8,9-DiHETrE	0.008 ± 0.002	0.007 ± 0.001	0.032 ± 0.019	0.005 ± 0.001	0.169
11,12-DiHETrE	0.055 ± 0.007	0.047 ± 0.007	0.137 ± 0.062	0.034 ± 0.004	0.125
14,15-DiHETrE	0.134 ± 0.024	0.105 ± 0.011	0.187 ± 0.067	0.078 ± 0.013	0.225
19,20-DiHDoPE	0.101 ± 0.034	0.043 ± 0.005	0.083 ± 0.021	0.035 ± 0.007	0.119
Dihydroxy FA:epoxy FA ratios					
9(10)DiHOME:EpOME	0.203 ± 0.025	0.187 ± 0.037	0.396 ± 0.147	0.164 ± 0.028	0.175
12(12)DiHOME:EpOME	0.479 ± 0.014	0.529 ± 0.166	0.267 ± 0.112	0.356 ± 0.148	0.460
5,6-DiHETrE:EpETrE	0.256 ± 0.040	0.194 ± 0.038	1.836 ± 1.436	0.292 ± 0.077	0.334
8,9-DiHETrE:EpETrE	0.600 ± 0.034	0.664 ± 0.112	1.340 ± 0.743	0.420 ± 0.118	0.351
11,12-DiHETrE:EpETrE	1.107 ± 0.161	1.359 ± 0.437	1.100 ± 0.511	1.237 ± 0.324	0.962
14,15-DiHETrE:EpETrE	5.030 ± 0.642	4.956 ± 1.413	3.900 ± 1.748	4.517 ± 1.444	0.933
19(20)-DiHDoPE:EpDPE	4.444 ± 0.858	1.930 ± 0.286	1.986 ± 0.683	1.988 ± 0.808	0.053
All DihydroxyFA:EpoxyFA	0.481 ± 0.044	0.439 ± 0.092	0.707 ± 0.328	0.408 ± 0.098	0.641

Data are expressed as the means ± SEM or ratio ± SEM. Units are given as nanograms per milligram protein.

EtOH, ethanol; FA, fatty acid, PF, pair-fed; PUFA, polyunsaturated fatty acid; TUCB, 4-[[*trans*-4-[[[[4-trifluoromethoxy phenyl]amino]carbonyl]-amino] cyclohexyl]oxy]-benzoic acid.

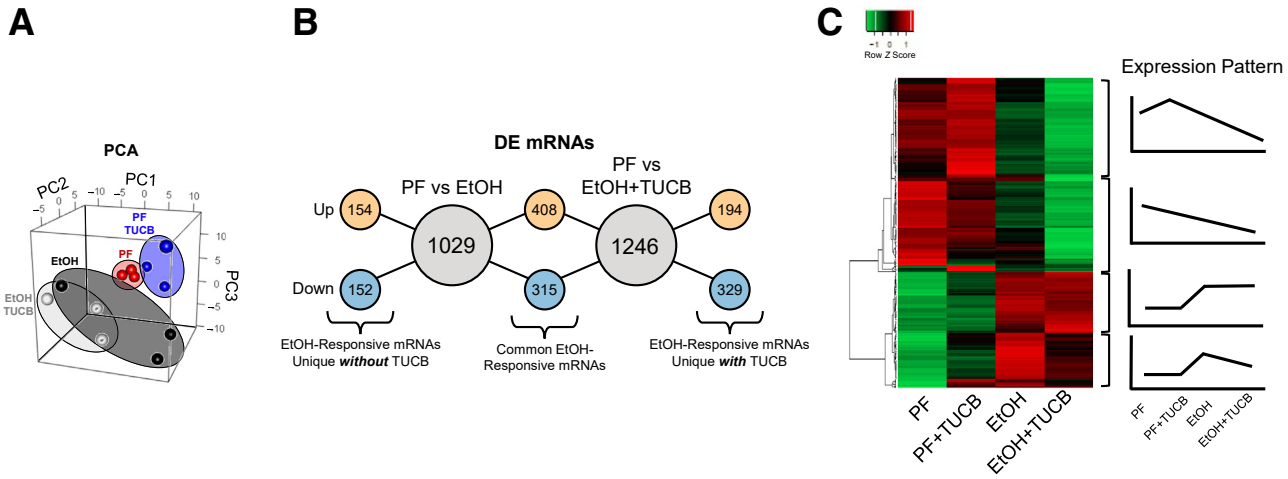

Figure 3 Liver RNA sequencing analysis. **A:** Principal component analysis (PCA) of all mRNA across the four groups. **B:** Summary of differentially expressed mRNAs across experimental groups. **C:** Heatmap of ethanol (EtOH)-responsive mRNAs unique with 4-[[*trans*-4-[[[[4-trifluoromethoxy phenyl]amino]carbonyl]-amino]cyclohexyl]oxy]-benzoic acid (TUCB) and graphical representation of patterns of expression. $n = 3$ animals per group. DE, differentially expressed; PC1, first principal component; PC2, second principal component; PC3, third principal component; PF, pair-fed.

Table 3 Significant DE mRNAs From the Direct EtOH Versus EtOH + TUCB Comparison

EtOH + TUCB versus EtOH significant DE mRNAs				
Gene symbol	Full gene name	$\log_2$ FC	Adjusted *P* value	Entrez Gene summary
Cxcl13	CXC Motif Chemokine Ligand 13	3.797	1.05×10^{-05}	B lymphocyte chemoattractant
Atp6v0a4	ATPase H+ Transporting V0 Subunit A4	3.721	2.11×10^{-06}	V-ATPase dependent acidification
Igdcc4	IG Superfamily DCC Subclass Member 4	2.551	9.86×10^{-07}	No function listed
Ins2	Insulin II	2.201	1.78×10^{-06}	Carbohydrate and lipid metabolism
Apcs	Amyloid P component, serum	1.809	1.25×10^{-06}	Protein chaperone
Tox2	TOX High Mobility Group Box Family Member 2	1.784	4.00×10^{-05}	Positive regulation of transcription
Ccnd1	Cyclin D1	1.525	4.77×10^{-07}	Positive regulation of cell cycle (G1 to S)
Fam81a	Family With Sequence Similarity 81 Member A	1.323	2.01×10^{-05}	No function listed
Armcx4	Armadillo Repeat Containing X-Linked 4	1.154	7.85×10^{-06}	No known function
Tro	Trophinin	−1.357	1.88×10^{-05}	Cell adhesion
Atp6v0d2	ATPase H+ Transporting V0 Subunit D2	−1.677	3.02×10^{-06}	Vacuolar acidification and transport
Gm15889	*Predicted gene*	−2.09	2.48×10^{-06}	Unknown
Cyp2c40	Cytochrome P450 Family 2 Subfamily C Member 40	−2.242	5.38×10^{-05}	Arachidonic acid metabolism
Trim43c	Tripartite Motif Containing 43	−2.522	1.77×10^{-05}	Ubiquitin protetin ligase
Cyp2b13	Cytochrome P450 Family 2 Subfamily B Member 13	−4.056	3.95×10^{-05}	Steroid and xenobiotic metabolism

All 15 significant DE mRNAs are listed in order of decreasing $\log_2$ FC. Entrez gene summaries were retrieved from *https://www.ncbi.nlm.nih.gov/gene* (last accessed November 30, 2022).

DE, differentially expressed; EtOH, ethanol; FC, fold change; TUCB, 4-[[*trans*-4-[[[[4-trifluoromethoxy phenyl]amino] carbonyl]-amino]cyclohexyl]oxy]-benzoic acid.

DhFAs as shown by the separation of groups (Figure 2B). Importantly, TUCB administration shifted this clustering back toward a PF-like phenotype, indicating a favorable shift in these sEH substrates and metabolites.

Characterization of the Transcriptional Responses to TUCB Administration in EtOH-Fed Mice

To gain a deeper mechanistic insight into TUCB-mediated attenuation of EtOH-induced liver injury, liver transcriptomic analysis (bulk RNA sequencing) was performed to identify novel transcripts and pathways associated with sEH inhibition. PCA of hepatic mRNAs revealed both an effect of EtOH and an effect of TUCB as evidenced by separation of the PF versus EtOH groups, as well as a separation of the PF versus PF + TUCB group and the EtOH versus EtOH + TUCB group (Figure 3A). The direct EtOH + TUCB versus EtOH comparison yielded 15 significant DE mRNAs, which likely represented the transcripts most highly associated with the attenuation of liver injury by sEH inhibition (Table 3). Among these DE mRNAs were up-regulated or down-regulated genes related to immunity [B-cell chemoattractant *Cxcl13* and host defense *Apcs* (*SAP/Pentraxin2*), both up], energy homeostasis

Table 4 Differential mRNA Expression Analysis Summary

Comparison	Up-regulated genes	Down-regulated genes	Total significantly differentially expressed genes
PF vs EtOH	562	467	1029
PF vs EtOH + TUCB	602	644	1246
PF + TUCB vs EtOH + TUCB	313	366	679
PF vs PF + TUCB	6	13	19
EtOH vs EtOH + TUCB	9	6	15

The number of differentially expressed mRNAs are provided for each statistical comparison.

EtOH, ethanol; PF, pair-fed; TUCB, 4-[[*trans*-4-[[[[4-trifluoromethoxy phenyl]amino]carbonyl]-amino]cyclohexyl]oxy]-benzoic acid.

Table 5 Free Nucleosides, Nucleotides, and Nucleoside Modifications

Metabolite	PF ($n = 6$)	PF + TUCB ($n = 6$)
Free nucleosides		
Uridine	103,810,193 ± 18,712,389	96,637,205 ± 18,323,766
Pseudouridine	8,435,630 ± 1,073,721	6,079,525 ± 1,296,377
Adenosine modifications		
m^1A	25,976,322 ± 3,879,743	28,383,736 ± 3,893,732
m^6A	5,762,702 ± 1,074,172	5,749,738 ± 379,927
m^6Am	2,742,774 ± 294,803	2,025,716 ± 290,571
i^6A	1,008,422 ± 95,278	1,259,956 ± 116,786
ms^2t^6A	44,678 ± 22,905	255,760 ± 184,244
N6-SAR	31,375,395 ± 11,910,484	24,816,169 ± 4,338,444
Cytidine modifications		
m^3C	20,695,247 ± 5,900,459	23,913,296 ± 4,947,220
m^5C	2,845,497 ± 761,209	3,642,990 ± 532,612
Cm	2,047,673 ± 450,840	2,065,092 ± 69,040
Guanosine modifications		
m^1G	5,655,331 ± 795,935	9,380,671 ± 3,667,779
Gm	3,255,811 ± 337,802	3,193,188 ± 270,811
Uridine modifications		
m^3U	658,222 ± 70,409	598,741 ± 81,134
m^5U	953,401 ± 171,121	932,628 ± 115,049
Um	190,066 ± 34,936	166,104 ± 16,887

(*table continues*)

Data are expressed as mean peak intensity ± SEM.

Cm, 2′-O-methylcytidine; EtOH, ethanol; Gm, 2′-O-methylguanosine; i^6A, N^6-isopentenyladenosine; m^1A, 1-methyladenosine; m^1G, 1-methylguanosine; m^3C, 3-methylcytidine; m^3U, 3-methyluridine; m^5C, 5-methylcytidine; m^5U, 5-methyluridine; m^6A, N^6-methyladenosine; m^6Am, N^6, 2′-O-dimethyladenosine; ms^2t^6A, 2-methylthio-N^6-threonylcarbamoyladenosine; N6-SAR, N6-succinyl adenosine; PF, pair-fed; TUCB, 4-[[*trans*-4-[[[[4-trifluoromethoxy phenyl]amino]carbonyl]-amino]cyclohexyl]oxy]-benzoic acid; Um, 2′-O-methyluridine.

(*Atp6v0a4* and *Atp6v0d2,* up and down, respectively), metabolic homeostasis (*Ins2,* up; cytochrome P450 enzymes *Cyp2c40* and *Cyp2b13*, down), transcriptional control (*Tox2*, up), cell cycle control (*Ccnd1*, up), cell adhesion (*Tro,* down), and protein ubiquitination (*Trim43c*, down). Further analysis identified 1029 DE mRNAs resulting from EtOH consumption (PF versus EtOH comparison, 562 up-regulated and 467 down-regulated) (Table 4). TUCB administration coupled with EtOH consumption led to a higher transcriptional plasticity with an increased number of DE mRNAs [PF versus EtOH + TUCB comparison, 1246 total (602 up-regulated and 644 down-regulated)]. All significant DE mRNAs for each comparison are listed in Supplemental Table S1.

When assessing the overlap between these two comparisons (PF versus EtOH compared with PF versus EtOH + TUCB), 723 DE mRNAs were shared (408 up and 315 down), leaving 523 EtOH-responsive mRNAs uniquely regulated by TUCB (194 up and 329 down) (Figure 3B and Supplemental Table S2). Next, the list of these 523 genes uniquely regulated by TUCB was manually analyzed. Expression of these genes fit into four distinct patterns as shown in Figure 3C. The pattern of most relevance to the improved by TUCB liver phenotype included 132 genes that were induced by EtOH and returned to near PF levels with TUCB. No instance in which a gene was down-regulated by EtOH, and then rescued by TUCB, was found. Among these 132 genes down-regulated by TUCB were those involved in a number of processes relevant to ALD, including apoptosis (*Gramd4*), inflammation (*Sqstm1*), fibrosis (*Peg3* and *Ptch2*), and cancer/cell cycle (*Pvr, Slc3a2, Gcnt4, Sema4c, Rhbdf1, Ccng2, Slc22a15, Myh10,* and *Snx24*).

Effects of TUCB on Modified RNA Base Abundance

Recent advances in the field suggest that reversible RNA modification may be an important regulatory mechanism for gene expression.[34] Thus, EtOH and EtOH + TUCB–mediated differences in cellular pools of free modified and unmodified liver nucleosides and nucleotides were further examined. There were 16 molecules total detected, including free nucleosides and numerous modifications of adenosine, uridine, guanosine, and cytidine; raw metabolite data are provided in Table 5. Among these molecules, PCA revealed a striking effect of EtOH (PF versus EtOH) and TUCB

Table 5 (*continued*)

EtOH ($n = 6$)	EtOH + TUCB ($n = 6$)	Analysis of variance *P* value
882,191 ± 273,924	618,694 ± 79,856	<0.0001
9,136,927 ± 259,510	1,593,050 ± 194,727	<0.0001
3,470,724 ± 647,550	998,070 ± 101,465	<0.0001
1,197,355,792 ± 124,620,719	480,245,357 ± 79,757,638	<0.0001
55,732,095 ± 6,505,620	106,125 ± 19,900	<0.0001
77,790,393 ± 11,658,497	365,025,309 ± 70,258,964	<0.0001
201,566 ± 134,453	428,655,514 ± 67,004,473	<0.0001
392,053,464 ± 63,791,188	70,673 ± 31,262	<0.0001
15,280,961 ± 5,837,493	1,148,541,160 ± 126,614,882	<0.0001
11,840,763 ± 3,773,616	83,263,354 ± 15,165,515	<0.0001
2,402,445 ± 188,633	2,829,553 ± 269,320	0.1979
449,744,845 ± 49,090,275	4,519,753 ± 466,284	<0.0001
862,927 ± 71,426	33,744,133 ± 7,507,068	<0.0001
44,639,573 ± 34,013,915	7,998,949 ± 3,943,654	0.0155
22,551,420 ± 6,299,069	5,704,729 ± 852,799	0.0002
2,033,952 ± 189,452	24,633,526 ± 4,685,488	<0.0001

treatment in EtOH-fed animals (EtOH versus EtOH + TUCB), whereas there were no changes by TUCB treatment in PF mice (PF versus PF + TUCB) (Figure 4A). Ward clustering (shown on the left edge of the heatmap) (Figure 4B) revealed two distinct sets of metabolites that were either increased or decreased in EtOH + TUCB versus EtOH (Figure 4, C and D, respectively). Notably, TUCB administration significantly reversed EtOH-induced changes in several metabolites, including 2′-O-methylguanosine, pseudouridine, N^6-methyladenosine, 5-methyluridine, 1-methylguanosine, N^6,2′-O-dimethyladenosine, and N^6-succinyl adenosine. Using RNA sequencing data, the gene expression profiles of RNA modifying enzymes (writers, erasers, and readers), which may be responsible for the aforementioned RNA modifications, were evaluated. Although there was a distinct effect of EtOH on these enzymes, there was only a weak effect of TUCB overall (Figure 5).

Discussion

The current study further documents the important role of sEH in the pathogenesis of liver diseases, specifically in ALD. A key finding of this study was that sEH inhibition by TUCB was efficacious in preventing the development of liver injury (as assessed by attenuated ALT levels) in male mice subjected to acute-on-chronic EtOH exposure. This observation is in line with a recent report,[14] which showed the beneficial effects of liver-specific genetic sEH ablation as well as sEH inhibition with an alternate sEH inhibitor, TPPU, in a similar experimental animal model in female mice. Attenuation of EtOH-induced liver injury in the liver-specific sEH$^{-/-}$ mice appeared more robust compared with pharmacologic inhibition with TPPU and was associated with decreased hepatic steatosis, reduced expression of several pro-inflammatory cytokines (eg, tumor necrosis factor-α, IL-1β, monocyte chemoattractant protein-1), decreased NF-κB phosphorylation in hepatocytes, and attenuated EtOH-induced oxidative and ER stress in the liver.[14] These findings were consistent with earlier reports establishing a pathogenic role for sEH in these processes.[6,12,18]

It is important to note that the current study revealed greater protection against EtOH-induced liver injury by TUCB versus TPPU[14] (based on ALT levels as a biomarker of liver injury), likely due to its higher potency in mice.[16,17] However, hepatic steatosis in EtOH-fed mice was not

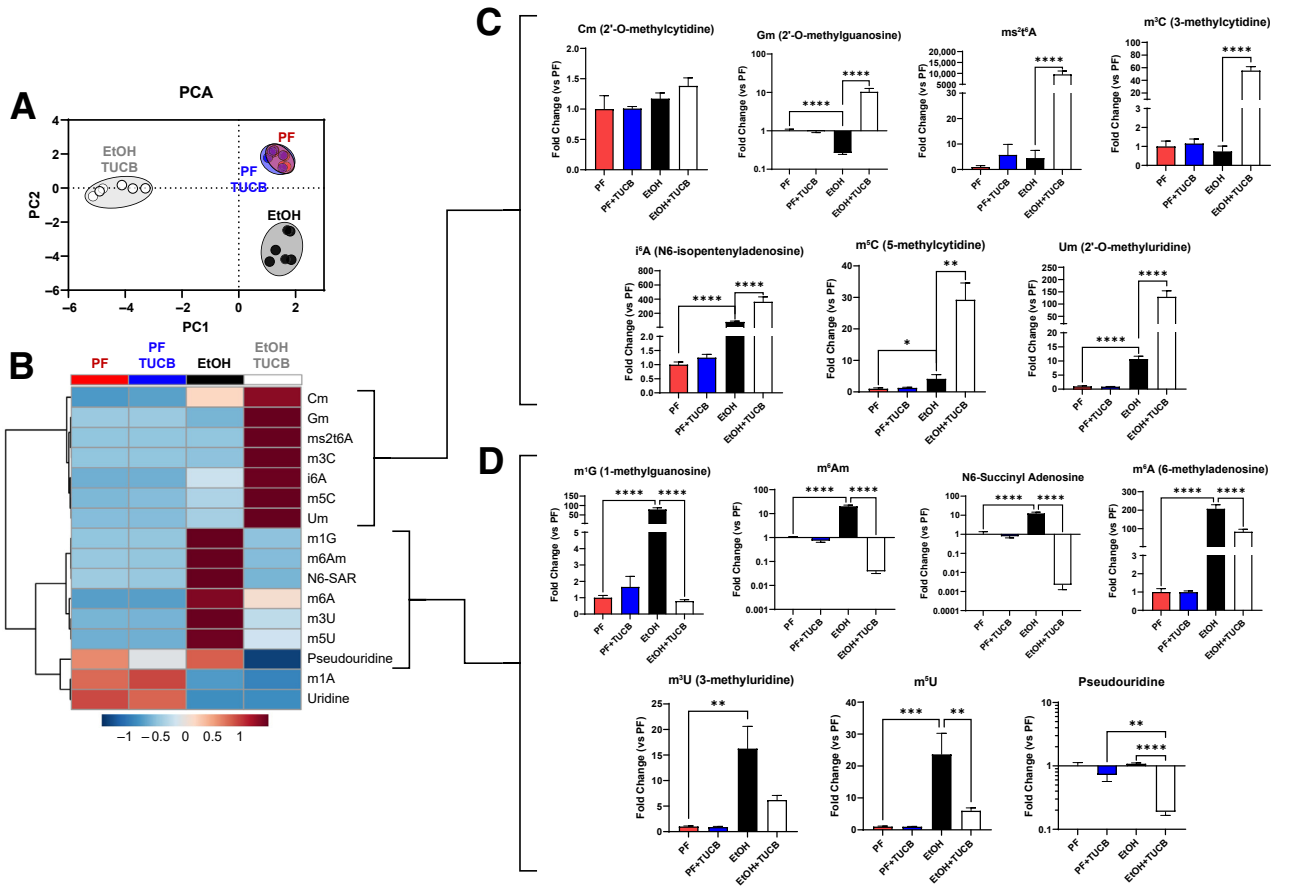

Figure 4 Epitranscriptomic modification of the liver RNA bases. **A:** Principal component analysis (PCA) of 16 detected RNA base modifications. **B:** Heatmap of all 16 base modifications with Ward clustering (left side, color scale represents *Z* score) showing two distinct groups of metabolites: **C:** Metabolites increased by 4-[[*trans*-4-[[[[4-trifluoromethoxy phenyl]amino]carbonyl]-amino]cyclohexyl]oxy]-benzoic acid (TUCB) in the ethanol (EtOH) versus EtOH + TUCB comparison. **D:** Metabolites decreased by TUCB in the EtOH versus EtOH + TUCB comparison. Data are expressed as mean fold change [compared with the pair-fed (PF) group] ± SEM. $n = 6$ animals per group. $^{*}P < 0.05$, $^{**}P < 0.01$, $^{***}P < 0.001$, $^{****}P < 0.0001$ (comparisons with no asterisk were not statistically significant). m^6Am, N^6, 2′-O-dimethyladenosine; ms^2t^6A, 2-methylthio-N^6-threonylcarbamoyladenosine; m^5U, 5-methyluridine.

affected by either TUCB or TPPU compared with complete sEH genetic deletion.[14] The limited effects of sEH inhibitors on liver steatosis caused by EtOH exposure could be in part due to potential residual sEH activity upon pharmacologic inhibition, or possible dissociation of hepatic steatosis from liver injury as previously observed in a similar animal model using *Trpv1*$^{-/-}$ mice.[35] Of note, both TUCB and TPPU ameliorated EtOH-induced hepatic ER stress, a significant contributor to liver injury and a hallmark of ALD.[36] Beneficial effects of EtOH inhibition on ER stress may be in part due to prevention of increases in DhFAs, such as dihydroxy-octadecenoic acids, which are able to enhance ER stress in various *in vitro* cell models, including hepatocytes.[12,37] However, unlike TPPU, TUCB had no effects on EtOH-induced hepatic oxidative stress. This observation requires additional investigation, as a previous study reported attenuation of hepatic oxidative stress by TUCB in a CCl_4-induced liver fibrosis model in rats.[18]

The next finding that TUCB treatment led to elevated levels of hepatic M2-type macrophages is of particular significance to the pathophysiology of ALD, as M2 macrophages, which possess anti-inflammatory, tissue repair, and regeneration capacity,[32,38] may promote the resolution of this disease. This TUCB-mediated increase in M2-type macrophages likely occurred due to enrichment of the pool of EpFAs, which have the ability to supress M1 and promote M2 macrophage polarization in various cells and tissues.[39,40]

Hepatic RNA sequencing analysis revealed several hepatic transcriptional changes, which may shed new light on the mechanisms contributing to attenuation of EtOH-induced liver injury by TUCB. TUCB treatment in EtOH-fed mice (the EtOH versus EtOH + TUCB comparison) led to 15 significant DE mRNAs associated with TUCB-mediated protection from liver injury. Among them were increased *Cxcl13*, a B-cell chemoattractant whose increased expression may compensate for the loss of B lymphocytes characteristic of both experimental and human ALD.[41] Elevation of *Apcs* expression may also contribute to the attenuation of EtOH-induced liver injury in our model given its role in phagocytosis of cell debris as well as its anti-inflammatory and antifibrotic properties.[42,43] Also

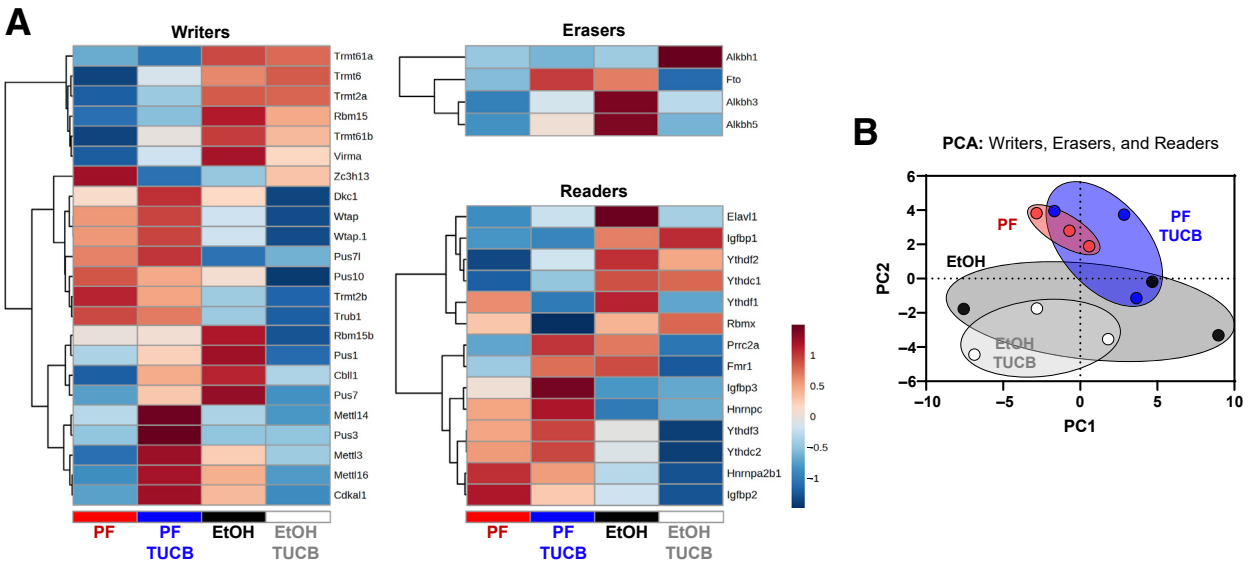

Figure 5 Gene expression of epitranscriptomic writers, erasers, and readers in the mRNA sequencing database. **A:** Heatmap with Ward clustering (left side, color scale represents *Z* score) for each category. **B:** Principal component analysis (PCA) for writers, erasers, and readers. $n = 6$ animals per group. EtOH, ethanol; PC1, first principal component; PC2, second principal component; PF, pair-fed; TUCB, 4-[[*trans*-4-[[[[4-trifluoromethoxy phenyl]amino]carbonyl]-amino]cyclohexyl]oxy]-benzoic acid.

increased were *Tox2*, a transcription factor that promotes the differentiation of natural killer cells,[44] which, in turn, play pleotropic roles in host defense in the liver,[45] and *Ccnd1*, which through noncanonical signaling was shown to suppress the development of hepatic steatosis.[46] Down-regulated transcripts included decreased cytochrome P450 enzymes such as *Cyp2b13*, previously shown to be associated with non−alcohol-associated fatty liver disease,[47] and *Cyp2c40*, whose subfamily contributes to the production of EpFAs.[48] Down-regulation of *Cyp2c40* may represent a negative feedback response to elevated EpFA levels caused by TUCB. Among the genes exclusively regulated by TUCB, there were several down-regulated mRNAs with possible relevance to ALD pathogenesis, including *Gramd4*, which has been previously shown to induce apoptosis,[49] a type of cell death often seen in ALD.[50] Down-regulation by TUCB of *Sqstm1* expression may be an additional mechanism by which it can ameliorate ALD, as SQSTM1 has been implicated in the promotion of M1-type macrophages,[51] elevated levels of which are often associated with ALD.[52] Furthermore, several genes linked to fibrosis were identified as being down-regulated by TUCB, including *Peg3* and *Ptch2*.

Although fibrosis is not typically found in the ALD model used for the current study, it is possible that early gene expression changes occur that may predispose the liver to fibrosis. Down-regulation of *Peg3* in hepatic stellate cells has been previously shown to decrease liver fibrosis in a mouse model of nonalcoholic steatohepatitis[53] and may play a similar role in advanced ALD. *Ptch2 is* the receptor for Hedgehog signaling, activation of which correlates to the severity of both ALD and nonalcoholic fatty liver disease.[54] Down-regulation of *Ptch2* would possibly lead to a decrease in overall Hedgehog signaling and lessening of liver damage. Lastly, among the TUCB down-regulated genes, there were also several that are linked to carcinogenesis, suggesting the possibility that TUCB may ultimately lessen the risk of developing hepatocellular carcinoma in more advanced ALD. It is important to note that the data obtained by RNA sequencing analysis are exploratory and need further confirmation and investigation.

Another important finding of the current study was related to reversible RNA base modification, termed "epitranscriptomics," a feature of mRNA biology that has recently garnered increasing scientific attention. While still a nascent field, accumulating evidence suggests that enzymatic chemical mRNA modification (particularly methylation) in both coding and noncoding regions can contribute to the regulation of processes such as pre-mRNA splicing, export, translation, and turnover, as reviewed thoroughly by Kumar and Mohapatra.[34] One of the most commonly studied epitranscriptomic modifications is N^6-methyladenosine, which causes destabilization of adenosine-uridine base pairing.[55] Previous studies linked this base modification, which was increased by EtOH and decreased by TUCB in our model, to increased risk of alcohol-associated hepatocellular carcinoma via its role in promoting cell proliferation and migration[56] and, more broadly, to the regulation of liver diseases in general.[57] Another robustly altered RNA base modification identified by our study was 2-methylthio-N^6-threonylcarbamoyladenosine, which is a tRNA modification that enhances the binding ability of tRNAs to ribosomes, improving translational fidelity.[58] Loss of 2-methylthio-N^6-threonylcarbamoyladenosine, which was increased greatly by TUCB in the current study, has been linked to the development of type 2 diabetes in mice.[59] Multiple other base

modifications increased or decreased by EtOH matched previously established trends in human AH patients[60] and were often reversed by TUCB. Little is known regarding many of these epitranscriptomic marks; future research is needed to address their molecular functions and how sEH inhibition, through EpFAs, alter their abundance.

There are some limitations to the current study, including that only male mice were studied. Although it complements a previous report,[14] which showed the beneficial effects of sEH deletion/inhibition in female mice, future studies are required to investigate the effects of sEH inhibition and underlying molecular mechanisms in both sexes. Next, the effects of sEH inhibition was determined on the hepatic transcriptome as a whole, rather than at the single-cell level, which would provide better understanding of the cell-specific responses revealing the possibility of developing cell-targeted sEH inhibition strategies. Nevertheless, evidence from the current study and a previously published report[14] suggest that both immune cells and hepatocytes may be involved in the response to sEH inhibition in ALD, as TUCB treatment resulted in an elevated hepatic M2 macrophage phenotype and sEH deletion in primary hepatocytes led to decreased EtOH-mediated NF-kB activation. The fact that sEH is expressed in virtually all tissues and cell types would also suggest that multiple cell types may play roles in the protective effect of sEH inhibition given that ALD is a complex pathology that involves multiple cell types and multiorgan interactions. Lastly, the epitranscriptomic approach measured only free cellular modified bases in whole-liver lysates, rather than at a transcript-specific level, which did not allow pairing of epitranscriptomic modifications to specific mRNAs.

In summary, this study showed the beneficial effects of sEH inhibition by TUCB in experimental EtOH-induced liver injury, highlighting the translational potential of sEH as a drug target for this disease. Novel TUCB-mediated hepatic transcriptional and epitranscriptomic changes identified in this report set the stage for future mechanistic studies exploring how sEH inhibition benefits ALD.

Acknowledgment

We thank Marion McClain for manuscript editing support.

Author Contributions

I.A.K. and J.B.W. conceptualized the study; J.B.W., J.E.H., Y.L.S., A.T.F., A.J., L.H., Z.D., and D.R.W. executed the study; X.Z., C.J.M., B.D.H., Z.D., and I.A.K. provided resources; J.B.W. wrote the original draft of the manuscript; J.B.W., J.E.H., D.R.W., B.D.H., C.J.M., X.Z., and I.A.K. reviewed and edited the manuscript; I.A.K. supervised the project; and J.B.W., C.J.M., and I.A.K. acquired funding.

Disclosure Statement

B.D.H. founded EicOsis Human Health, currently in clinical trials of sEH inhibitors.

Supplemental Data

Supplemental material for this article can be found at *http://doi.org/10.1016/j.ajpath.2023.09.016*.

References

1. Seitz HK, Bataller R, Cortez-Pinto H, Gao B, Gual A, Lackner C, Mathurin P, Mueller S, Szabo G, Tsukamoto H: Alcoholic liver disease [Erratum appeared in Nat Rev Dis Primers 2018;4:18]. Nat Rev Dis Primers 2018, 4:16
2. Hosseini N, Shor J, Szabo G: Alcoholic hepatitis: a review. Alcohol Alcohol 2019, 54:408−416
3. Thursz M, Morgan TR: Treatment of severe alcoholic hepatitis. Gastroenterology 2016, 150:1823−1834
4. Thompson JA, Martinson N, Martinson M: Mortality and costs associated with alcoholic hepatitis: a claims analysis of a commercially insured population. Alcohol 2018, 71:57−63
5. Warner J, Hardesty J, Zirnheld K, McClain C, Warner D, Kirpich I: Soluble epoxide hydrolase inhibition in liver diseases: a review of current research and knowledge gaps. Biology (Basel) 2020, 9:124
6. Node K, Huo Y, Ruan X, Yang B, Spiecker M, Ley K, Zeldin DC, Liao JK: Anti-inflammatory properties of cytochrome P450 epoxygenase-derived eicosanoids. Science 1999, 285:1276−1279
7. Spector AA: Arachidonic acid cytochrome P450 epoxygenase pathway. J Lipid Res 2009, 50 Suppl:S52−S56
8. Wray JA, Sugden MC, Zeldin DC, Greenwood GK, Samsuddin S, Miller-Degraff L, Bradbury JA, Holness MJ, Warner TD, Bishop-Bailey D: The epoxygenases CYP2J2 activates the nuclear receptor PPARalpha in vitro and in vivo. PLoS One 2009, 4:e7421
9. Liu Y, Zhang Y, Schmelzer K, Lee T-S, Fang X, Zhu Y, Spector AA, Gill S, Morisseau C, Hammock BD, Shyy J-YJ: The antiinflammatory effect of laminar flow: the role of PPARgamma, epoxyeicosatrienoic acids, and soluble epoxide hydrolase. Proc Natl Acad Sci U S A 2005, 102:16747−16752
10. Matsumoto N, Singh N, Lee KS, Barnych B, Morisseau C, Hammock BD: The epoxy fatty acid pathway enhances cAMP in mammalian cells through multiple mechanisms. Prostaglandins Other Lipid Mediat 2022, 162:106662
11. López-Vicario C, Alcaraz-Quiles J, García-Alonso V, Rius B, Hwang SH, Titos E, Lopategi A, Hammock BD, Arroyo V, Clària J: Inhibition of soluble epoxide hydrolase modulates inflammation and autophagy in obese adipose tissue and liver: role for omega-3 epoxides. Proc Natl Acad Sci U S A 2015, 112:536−541
12. Bettaieb A, Nagata N, AbouBechara D, Chahed S, Morisseau C, Hammock BD, Haj FG: Soluble epoxide hydrolase deficiency or inhibition attenuates diet-induced endoplasmic reticulum stress in liver and adipose tissue. J Biol Chem 2013, 288:14189−14199
13. Warner D, Vatsalya V, Zirnheld KH, Warner JB, Hardesty JE, Umhau JC, McClain CJ, Maddipati K, Kirpich IA: Linoleic acid-derived oxylipins differentiate early stage alcoholic hepatitis from mild alcohol-associated liver injury. Hepatol Commun 2021, 5:947−960
14. Mello A, Hsu M-F, Koike S, Chu B, Cheng J, Yang J, Morisseau C, Torok NJ, Hammock BD, Haj FG: Soluble epoxide hydrolase hepatic deficiency ameliorates alcohol-associated liver disease. Cell Mol Gastroenterol Hepatol 2021, 11:815−830

15. Bertola A, Mathews S, Ki SH, Wang H, Gao B: Mouse model of chronic and binge ethanol feeding (the NIAAA model). Nat Protoc 2013, 8:627−637
16. Kodani SD, Bhakta S, Hwang SH, Pakhomova S, Newcomer ME, Morisseau C, Hammock BD: Identification and optimization of soluble epoxide hydrolase inhibitors with dual potency towards fatty acid amide hydrolase. Bioorg Med Chem Lett 2018, 28:762−768
17. Liang Z, Zhang B, Xu M, Morisseau C, Hwang SH, Hammock BD, Li QX: 1-Trifluoromethoxyphenyl-3-(1-propionylpiperidin-4-yl) urea, a selective and potent dual inhibitor of soluble epoxide hydrolase and p38 kinase intervenes in Alzheimer's signaling in human nerve cells. ACS Chem Neurosci 2019, 10:4018−4030
18. Zhang C-H, Zheng L, Gui L, Lin J-Y, Zhu Y-M, Deng W-S, Luo M: Soluble epoxide hydrolase inhibition with t-TUCB alleviates liver fibrosis and portal pressure in carbon tetrachloride-induced cirrhosis in rats. Clin Res Hepatol Gastroenterol 2018, 42:118−125
19. Deng W, Zhu Y, Lin J, Zheng L, Zhang C, Luo M: Inhibition of soluble epoxide hydrolase lowers portal hypertension in cirrhotic rats by ameliorating endothelial dysfunction and liver fibrosis. Prostaglandins Other Lipid Mediat 2017, 131:67−74
20. Kirpich IA, Gobejishvili LN, Bon Homme M, Waigel S, Cave M, Arteel G, Barve SS, McClain CJ, Deaciuc IV: Integrated hepatic transcriptome and proteome analysis of mice with high-fat diet-induced nonalcoholic fatty liver disease. J Nutr Biochem 2011, 22: 38−45
21. Warner DR, Warner JB, Hardesty JE, Song YL, Chen C-Y, Chen Z, Kang JX, McClain CJ, Kirpich IA: Beneficial effects of an endogenous enrichment in n3-PUFAs on Wnt signaling are associated with attenuation of alcohol-mediated liver disease in mice. FASEB J 2021, 35:e21377
22. Sun R, Gu X, Lei C, Chen L, Chu S, Xu G, Doll MA, Tan Y, Feng W, Siskind L, McClain CJ, Deng Z: Neutral ceramidase-dependent regulation of macrophage metabolism directs intestinal immune homeostasis and controls enteric infection. Cell Rep 2022, 38:110560
23. Chen L, Sun R, Lei C, Xu Z, Song Y, Deng Z: Alcohol-mediated susceptibility to lung fibrosis is associated with group 2 innate lymphoid cells in mice. Front Immunol 2023, 14:1178498
24. Love MI, Huber W, Anders S: Moderated estimation of fold change and dispersion for RNA-seq data with DESeq2. Genome Biol 2014, 15:550
25. Shannon P, Markiel A, Ozier O, Baliga NS, Wang JT, Ramage D, Amin N, Schwikowski B, Ideker T: Cytoscape: a software environment for integrated models of biomolecular interaction networks. Genome Res 2003, 13:2498−2504
26. He L, Li F, Yin X, Bohman P, Kim S, McClain CJ, Feng W, Zhang X: Profiling of polar metabolites in mouse feces using four analytical platforms to study the effects of cathelicidin-related antimicrobial peptide in alcoholic liver disease. J Proteome Res 2019, 18:2875−2884
27. He L, Wei X, Ma X, Yin X, Song M, Donninger H, Yaddanapudi K, McClain CJ, Zhang X: Simultaneous quantification of nucleosides and nucleotides from biological samples. J Am Soc Mass Spectrom 2019, 30:987−1000
28. Bertola A, Park O, Gao B: Chronic plus binge ethanol feeding synergistically induces neutrophil infiltration and liver injury in mice: a critical role for E-selectin. Hepatology 2013, 58:1814−1823
29. Ju C, Mandrekar P: Macrophages and alcohol-related liver inflammation. Alcohol Res 2015, 37:251−262
30. Galicia-Moreno M, Gutiérrez-Reyes G: The role of oxidative stress in the development of alcoholic liver disease. Rev Gastroenterol Mex 2014, 79:135−144
31. Ajoolabady A, Kaplowitz N, Lebeaupin C, Kroemer G, Kaufman RJ, Malhi H, Ren J: Endoplasmic reticulum stress in liver diseases. Hepatology 2023, 77:619−639
32. Yu Y, Yue Z, Xu M, Zhang M, Shen X, Ma Z, Li J, Xie X: Macrophages play a key role in tissue repair and regeneration. PeerJ 2022, 10:e14053
33. Nassir F, Ibdah JA: Role of mitochondria in alcoholic liver disease. World J Gastroenterol 2014, 20:2136−2142
34. Kumar S, Mohapatra T: Deciphering epitranscriptome: modification of mRNA bases provides a new perspective for post-transcriptional regulation of gene expression. Front Cell Dev Biol 2021, 9:628415
35. Liu H, Beier JI, Arteel GE, Ramsden CE, Feldstein AE, McClain CJ, Kirpich IA: Transient receptor potential vanilloid 1 gene deficiency ameliorates hepatic injury in a mouse model of chronic binge alcohol-induced alcoholic liver disease. Am J Pathol 2015, 185:43−54
36. Park SH, Seo W, Xu M-J, Mackowiak B, Lin Y, He Y, Fu Y, Hwang S, Kim S-J, Guan Y, Feng D, Yu L, Lehner R, Liangpunsakul S, Gao B: Ethanol and its nonoxidative metabolites promote acute liver injury by inducing ER stress, adipocyte death, and lipolysis. Cell Mol Gastroenterol Hepatol 2023, 15:281−306
37. Wang W, Wagner KM, Wang Y, Singh N, Yang J, He Q, Morisseau C, Hammock BD: Soluble epoxide hydrolase contributes to cell senescence and ER stress in aging mice colon. Int J Mol Sci 2023, 24:4570
38. Lee WJ, Tateya S, Cheng AM, Rizzo-DeLeon N, Wang NF, Handa P, Wilson CL, Clowes AW, Sweet IR, Bomsztyk K, Schwartz MW, Kim F: M2 macrophage polarization mediates anti-inflammatory effects of endothelial nitric oxide signaling. Diabetes 2015, 64: 2836−2846
39. Abdalla HB, Alvarez C, Wu Y-C, Rojas P, Hammock BD, Maddipati KR, Trindade-da-Silva CA, Soares MQS, Clemente-Napimoga JT, Kantarci A, Napimoga MH, Van Dyke TE: Soluble epoxide hydrolase inhibition enhances production of specialized pro-resolving lipid mediator and promotes macrophage plasticity. Br J Pharmacol 2023, 180:1597−1615
40. Dai M, Wu L, Wang P, Wen Z, Xu X, Wang DW: CYP2J2 and its metabolites EETs attenuate insulin resistance via regulating macrophage polarization in adipose tissue. Sci Rep 2017, 7:46743
41. Almeida J, Polvorosa MA, Gonzalez-Quintela A, Madruga I, Marcos M, Peréz-Nieto MA, Hernandez-Cerceño ML, Orfao A, Laso FJ: Altered distribution of peripheral blood maturation-associated B-cell subsets in chronic alcoholism. Alcohol Clin Exp Res 2015, 39:1476−1484
42. Nakagawa N, Barron L, Gomez IG, Johnson BG, Roach AM, Kameoka S, Jack RM, Lupher ML Jr, Gharib SA, Duffield JS: Pentraxin-2 suppresses c-Jun/AP-1 signaling to inhibit progressive fibrotic disease. JCI Insight 2016, 1:e87446
43. Cox N, Pilling D, Gomer RH: Serum amyloid P: a systemic regulator of the innate immune response. J Leukoc Biol 2014, 96:739−743
44. Vong QP, Leung WH, Houston J, Li Y, Rooney B, Holladay M, Oostendorp RAJ, Leung W: TOX2 regulates human natural killer cell development by controlling T-BET expression. Blood 2014, 124: 3905−3913
45. Tian Z, Chen Y, Gao B: Natural killer cells in liver disease. Hepatology 2013, 57:1654−1662
46. Hanse EA, Mashek DG, Becker JR, Solmonson AD, Mullany LK, Mashek MT, Towle HC, Chau AT, Albrecht JH: Cyclin D1 inhibits hepatic lipogenesis via repression of carbohydrate response element binding protein and hepatocyte nuclear factor 4[alpha]. Cell Cycle 2012, 11:2681−2690
47. Heintz MM, McRee R, Kumar R, Baldwin WS: Gender differences in diet-induced steatotic disease in Cyp2b-null mice. PLoS One 2020, 15:e0229896
48. Frömel T, Kohlstedt K, Popp R, Yin X, Awwad K, Barbosa-Sicard E, Thomas AC, Lieberz R, Mayr M, Fleming I: Cytochrome P4502S1: a novel monocyte/macrophage fatty acid epoxygenase in human atherosclerotic plaques. Basic Res Cardiol 2013, 108:319
49. John K, Alla V, Meier C, Pützer BM: GRAMD4 mimics p53 and mediates the apoptotic function of p73 at mitochondria. Cell Death Differ 2011, 18:874−886
50. Miyata T, Nagy LE: Programmed cell death in alcohol-associated liver disease. Clin Mol Hepatol 2020, 26:618−625
51. Zhou B, Liu J, Zeng L, Zhu S, Wang H, Billiar TR, Kroemer G, Klionsky DJ, Zeh HJ, Jiang J, Tang D, Kang R: Extracellular

SQSTM1 mediates bacterial septic death in mice through insulin receptor signalling. Nat Microbiol 2020, 5:1576−1587
52. Wan J, Benkdane M, Teixeira-Clerc F, Bonnafous S, Louvet A, Lafdil F, Pecker F, Tran A, Gual P, Mallat A, Lotersztajn S, Pavoine C: M2 Kupffer cells promote M1 Kupffer cell apoptosis: a protective mechanism against alcoholic and nonalcoholic fatty liver disease. Hepatology 2014, 59:130−142
53. Zhang Z, Wen H, Peng B, Weng J, Zeng F: Downregulated microRNA-129-5p by long non-coding RNA NEAT1 upregulates PEG3 expression to aggravate non-alcoholic steatohepatitis. Front Genet 2020, 11:563265
54. Machado MV, Diehl AM: Hedgehog signalling in liver pathophysiology. J Hepatol 2018, 68:550−562
55. Roost C, Lynch SR, Batista PJ, Qu K, Chang HY, Kool ET: Structure and thermodynamics of N6-methyladenosine in RNA: a spring-loaded base modification. J Am Chem Soc 2015, 137:2107−2115
56. Chen M, Wei L, Law C-T, Tsang FH-C, Shen J, Cheng CL-H, Tsang L-H, Ho DW-H, Chiu DK-C, Lee JM-F, Wong CC-L, Ng IO-L, Wong C-M: RNA N6-methyladenosine methyltransferase-like 3 promotes liver cancer progression through YTHDF2-dependent posttranscriptional silencing of SOCS2. Hepatology 2018, 67:2254−2270
57. Xu K, Sun Y, Sheng B, Zheng Y, Wu X, Xu K: Role of identified RNA N6-methyladenosine methylation in liver. Anal Biochem 2019, 578:45−50
58. Arragain S, Handelman SK, Forouhar F, Wei F-Y, Tomizawa K, Hunt JF, Douki T, Fontecave M, Mulliez E, Atta M: Identification of eukaryotic and prokaryotic methylthiotransferase for biosynthesis of 2-methylthio-N6-threonylcarbamoyladenosine in tRNA. J Biol Chem 2010, 285:28425−28433
59. Wei F-Y, Suzuki T, Watanabe S, Kimura S, Kaitsuka T, Fujimura A, Matsui H, Atta M, Michiue H, Fontecave M, Yamagata K, Suzuki T, Tomizawa K: Deficit of tRNA(Lys) modification by Cdkal1 causes the development of type 2 diabetes in mice. J Clin Invest 2011, 121:3598−3608
60. He L, Vatsalya V, Ma X, Klinge CM, Cave MC, Feng W, McClain CJ, Zhang X: Metabolic analysis of nucleosides/bases in the urine and serum of patients with alcohol-associated liver disease. Metabolites 2022, 12:1187